Tomography of full sawtooth crashes on the Tokamak Fusion Test Reactor

Y. Nagayama
National Institute for Fusion Science, Nagoya 464-01, Japan

M. Yamada, W. Park, E. D. Fredrickson, A. C. Janos, K. M. McGuire, and G. Taylor
Plasma Physics Laboratory, Princeton University, Princeton, New Jersey 08543

(Received 31 October 1995; accepted 30 January 1996)

Full sawtooth crashes in high temperature plasmas have been investigated on the Tokamak Fusion Test Reactor (TFTR) [Plasma Phys. Controlled Fusion **33,** 1509 (1991)]. A strong asymmetry in the direction of major radius, a feature of the ballooning mode, and a remaining $m=1$ region after the crash have been observed with electron cyclotron emission image reconstructions. The TFTR data is not consistent with two-dimensional (2-D) models; it rather suggests a three-dimensional (3-D) localized reconnection arising on the bad curvature side. This process explains the phenomenon of fast heat transfer which keeps the condition $q_0<1$. © *1996 American Institute of Physics.* [S1070-664X(96)01405-9]

I. INTRODUCTION

The sawtooth oscillation, which is characterized by a periodic fast heat loss in the core plasma region, is a well known magnetohydrodynamic (MHD) nonlinear phenomenon in tokamak plasmas. No comprehensive model has yet been developed to explain the experimental observations. Kadomtsev's full reconnection model[1] is a standard two-dimensional (2-D) model, which explains the full sawtooth crash as follows: first the $m=1/n=1$ tearing mode grows and the crescent shaped $m=1$ magnetic island grows, where m and n are the poloidal and toroidal mode numbers of the helical structure, respectively; second the reconnection takes place at the X-point of the island that is on the $q=1$ surface; finally the field line of the core region is reconnected to that of the outer region. So, the heat conduction and the particle convection along the field line, which are much greater than that across the flux surface, causes the very fast transfer of the heat and particles across the $q=1$ surface. This model is consistent with soft x-ray tomography,[2] but it is inconsistent with q profile measurements.[3] It has been suggested that a three-dimensional (3-D) reconnection[4] plays an important role in the sawtooth crash.[5]

Various types of sawtooth oscillations have been observed on the Tokamak Fusion Test Reactor (TFTR).[6] There are two types of crashes: the full sawtooth crash and the partial sawtooth crash. The full crash is usually called the sawtooth crash. Before the crash, the pre-cursor oscillation and after the crash the post-cursor oscillation are observed. A newly observed oscillation named ''mid-cursor'' will be described in this paper. Sawtooth oscillations on TFTR are a combination of these crashes and oscillations. Observed crash time varies continuously from 40 μs to 2 ms. Since the plasma rotation is slow, fast crashes have not been analyzed in ion cyclotron radio frequency heated (ICRH) plasmas and in L-mode plasmas. The fast sawtooth crash (100 μs) in the hot ion mode plasma can be analyzed because of the fast plasma rotation, and the result is similar to the slow crash. In this paper, the full sawtooth crashes in hot ion mode (high β) plasma, in the ICRH (medium β) plasma and in the Ohmic (low β) plasma will be investigated. The pre-cursor, post-cursor and mid-cursor with the full crash are also analyzed so that the most full crashes on TFTR will be described in this paper.

Detailed analysis of the sawtooth crash has been performed on TFTR.[6–8] Observations of the sawtooth crash in the high β discharges on TFTR can be summarized as follows: (1) transfer of both particles and heat is fast;[6] (2) a circular hot spot shrinks and a crescent island expands;[6] (3) the condition $q_0<1$ is preserved;[7] (4) the amount of flux change is about 20%–30% of that expected by the full reconnection model.[8] In this paper, we address the sawtooth crash in TFTR plasmas using electron cyclotron emission (ECE) image reconstruction, and there will be four additional results: (5) the reconnection happens on the bad curvature side (the outboard side); (6) the hot spot has a feature of the ballooning mode, which is the strong in-out asymmetry in the direction of major radius; (7) a substantial fraction of the $m=1$ helical current remains in the original hot spot region after the sawtooth crash; (8) a cold bubble precursor is observed but it causes a partial crash. The TFTR data suggest a localized reconnection on the bad curvature side, which is a 3-D process. This process is consistent with the phenomenon of fast heat transfer, while still keeping $q_0<1$ during the sawtooth crash.

II. SAWTOOTH CRASH

A. Sawtooth crash in high β plasmas

An example of a slow sawtooth crash in the hot-ion mode is shown in Figs. 1–5. Figure 1 shows the time evolution of the plasma parameters and ECE signals of a beam heated TFTR plasma with $\beta_p=0.95$, $q_a=4$, $B_t=4.8$ T, $I_p=1.58$ MA, $R=245$ cm and $a=80$ cm. The crash time is 1.5 ms. Figure 2 shows the time evolution of the electron temperature profile and the perturbation profile on the midplane. The electron temperature profile is measured with a 20 channel grating polychromator[9] covering $R=220-340$ cm with a channel separation of 6 cm. Here, the ECE (perturbation) is defined as $\delta T_e=T_e(r,t)-<T_e(r,t)>$, where the bracket indicates the time average over one cycle of the $m=1$ oscillation. The contour plot of δT_e provides a visual

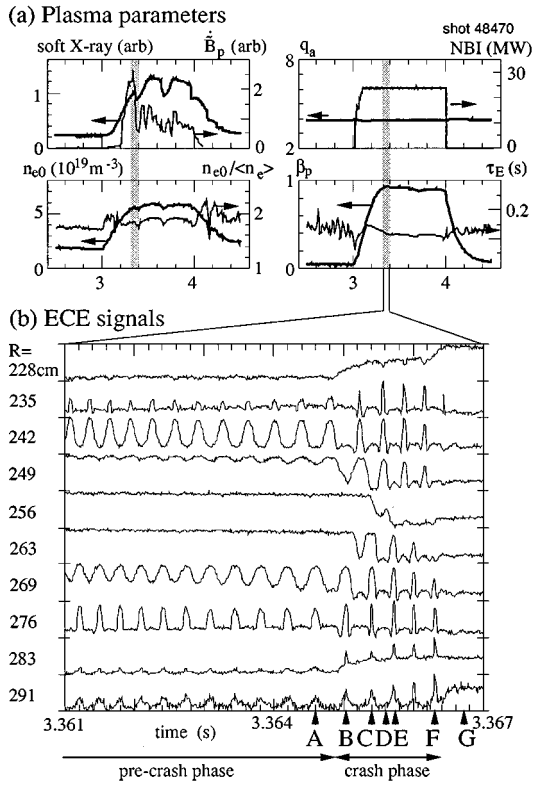

FIG. 1. Time evolution of soft x-ray, central plasma density (n_{e0}), density peaking parameter ($n_{e0}/\langle n_e\rangle$), q_a (cylindrical), NBI power, poloidal beta (β_p) and energy confinement time (τ_E) in the case of slow sawtooth crash in a hot ion mode plasma. (b) The ECE signals of a slow sawtooth crash in the hot ion mode plasma.

representation of MHD instabilities. As the mode rotates rigidly in the toroidal direction, the time corresponds to the toroidal angle. The contour plot of one cycle corresponds to the temperature profile on the mid-plane of the torus over 360° in the toroidal direction. It is often observed that the

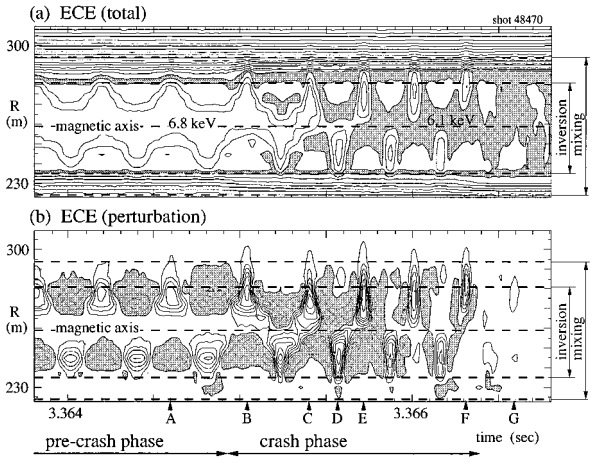

FIG. 2. (a) Time evolution of electron temperature profile during the slow sawtooth crash in a NBI heated plasma. The contour step size is 250 eV. The hatched region indicates $T_e = 6-6.25$ keV. (b) Time evolution of perturbation in the electron temperature profiles. The contour step size is 100 eV. The hatched region indicates negative value. The magnetic axis, the position of the inversion radius and the mixing radius are also shown.

$m=1$ mode is slowly growing before the sawtooth crash. This is called the pre-crash phase. The pre-crash phase is sustained for 70 ms, and the crash phase lasts for 2 ms. The mode patterns are different in the pre-crash phase and in the crash phase. In the pre-crash phase, the shape of the hot spot is rounded and stays inside the inversion radius. In the crash phase, δT_e on the bad curvature side extends to the mixing radius. This strong in-out asymmetry in the direction of major radius shows that the perturbation is localized in both poloidal and toroidal directions, because the perturbation has an $m=1/n=1$ helical structure. This extension is very narrow, thus it is very localized in the toroidal direction (compare time A and time C). In the early stage of the crash-phase, it is not localized because the round shaped $m=1$ pattern exists inside the inversion radius (times B, C). The narrowing is not due to a frequency change.

Figure 3 shows a series of contour plots of the ECE image reconstructions during the crash phase. The 2-D electron temperature profile in the poloidal plasma cross-section is obtained using the fast toroidal rotation of the MHD mode. The reconstruction technique and its reliability are discussed in a previous paper.[10] The main conclusions are as follows: (1) the MHD mode rotates rigidly even if the impurity rotation velocity varies in the radial position; (2) the reconstruction error is small if the crash time is longer than 2 rotational periods. The present sawtooth crash takes 5 rotational periods, so the reconstruction should have very small artifacts. The ECE (difference) is defined as $\Delta T_e(r,\theta) = T_e(r,\theta) - [T_e(r,\theta)]$, where $\mathrm{Min}[T_e(r,t)]$ is the minimum over a full time interval of the sawtooth period.[11] The contour plot of ΔT_e provides a visual presentation of the heat transfer from the inside to the outside of the inversion radius during the sawtooth crash process. The inversion radius and the mixing radius are indicated in Fig. 4. The definition of those radii is slightly different from the original definition by Kadomtsev.[1] The circular-shaped ΔT_e pattern is located in the core region before the crash (frame A), and ΔT_e gradually grows on a ring-shaped region between the inversion radius and the mixing radius (frames B-G). The ring-shaped pattern is generated by reconnections. The hot spot shape is circular in the pre-crash phase (frame A), and it is radially elongated in the crash phase (frames B, C). The spatial resolution (12° poloidally and 6 cm radially) is sufficient to distinguish the shape of the hot spot. This radially elongated shape shows that the perturbation is localized in the poloidal direction. This is probably due to a ballooning mode with high m Fourier components. Without such a mode, the shape of the hot spot tends to be elongated in the poloidal direction.[12]

In Fig. 5, we compare the island structure when the hot spot is on the good curvature side and on the bad curvature side. The δT_e of the hot spot extends to the mixing radius on the bad curvature side, while its boundary on the good curvature side is between the inversion radius and the mixing radius. In the image reconstruction of the ECE (difference), the hot spot is weakly coupled with the ring-shaped region on the good curvature side. On the bad curvature side, the hot spot overlaps onto the ring-shaped region. These significant in-out asymmetries in the ΔT_e and the δT_e contour plots suggest that the heat is escaping from the hot spot to

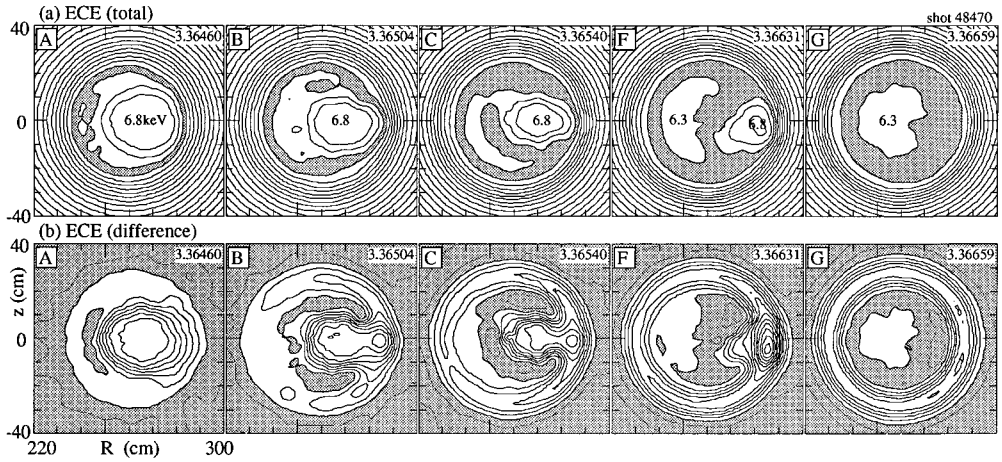

FIG. 3. (a) Series of ECE images when the hot spot is on the bad curvature side. The contour step size is 250 eV. The hatched region indicates $T_e = 6 - 6.25$ keV. (b) Reconstruction of the temperature difference. The contour step size is 100 eV and the hatched region indicates less than 300 eV. The numbers on the left shoulder of the figures indicate the reconstruction time in seconds. The capital letters on the left of the figures correspond to the alphabets in Fig. 2.

the ring shaped region on the bad curvature side, thus the reconnection is mainly on the bad curvature side. This shows that the reconnection is localized in both poloidal and toroidal directions, considering that the hot spot has an $m = 1/n = 1$ helical structure.

B. Sawtooth crash in ICRH plasmas

An example of a sawtooth crash in ICRH plasma is shown in Figs. 6–7. Figure 6 shows the time evolution of the plasma parameters and ECE signals of an ICRH heated TFTR plasma with $\beta_p = 0.4$, $q_a = 4$, $B_t = 3.5$ T, $I_p = 1.4$ MA, $R = 260$ cm and $a = 95$ cm. The crash time is 2 ms. Figure 7 shows the ECE image reconstructions during a slow, full sawtooth crash. In the early stage of the crash, the crescent shaped-island grows, and the size of the circular hot spot reduces (see Fig. 7 [B]). However, an isothermal contour (thick contour) around the hot spot does not shrink much, while the temperature at the hot spot decreases. This indicates that the region between the hot spot and the island is warmer than the island. The $m = 1$ warm region surrounded by the thick contour exists at the end of the crash (see Fig. 7 [F]).

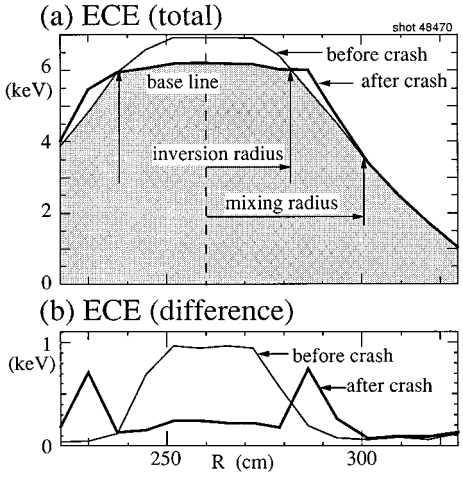

FIG. 4. Definition of the inversion and mixing radii. The profile with hutched area is the base line (Min$[T_e(r,t)]$).

C. Sawtooth crash in Ohmic plasmas

An example of a sawtooth crash in Ohmic plasma is shown in Figs. 8–9. The plasma parameters of this shot are

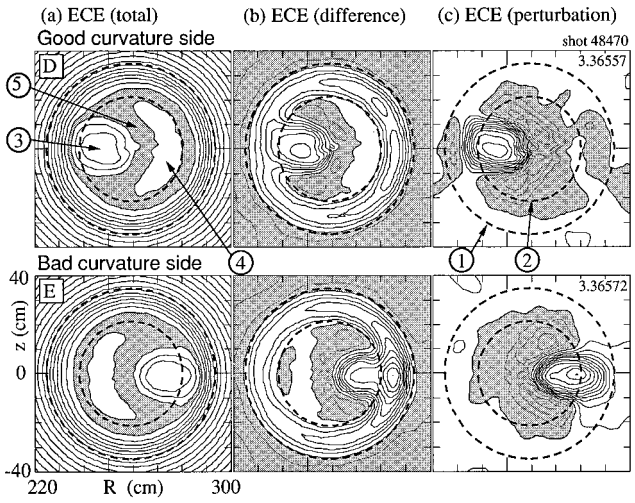

FIG. 5. Comparison of the reconstructed ECE images when the hot spot is on the good curvature side and on the bad curvature side. (a) The contour plot of the electron temperature profile; the contour step size is 250 eV, and the hatched region indicates $T_e = 6 - 6.25$ keV. (b) The contour plot of the temperature difference; the contour step size is 100 eV and the hatched region indicates less than 300 eV. (c) The contour plot of the perturbation of the electron temperature; the contour step size is 60 eV. The dashed circles indicate (1) the mixing radius, (2) the inversion radius. The regions indicate (3) the hot spot, (4) the island, and (5) the cool region between the hot spot and the island. The capital letters on the left of the figures correspond to the alphabets in Fig. 2.

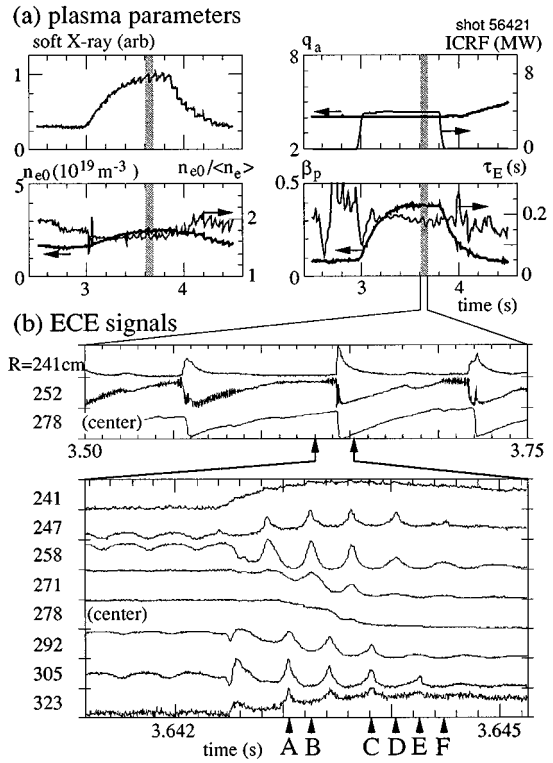

FIG. 6. (a) Time evolution of soft x-ray, central plasma density (n_{e0}), density peaking parameter ($n_{e0}/\langle n_e\rangle$), q_a (cylindrical), NBI power, poloidal beta (β_p) and energy confinement time (τ_E) in the case of slow sawtooth crash in ICRH heated plasma. (b) The soft x-ray and ECE signals of a slow sawtooth crash in the ICRH heated plasma.

following: $n_{e0}=3.5\times10^{19}$ m^{-3}, $n_{e0}/<n_e=1.8$, $q_a=3.8$, $\beta_p=0.11$ and $\tau_E=0.25$ s. The crash time is 1.2 ms. The ECE signals are shown in Fig. 8. A series of contour plots of the ECE reconstructions are shown at the moments indicated by the letters in Fig. 9(a). The hot spot shape is not exactly circular, but the hot spot shrinks and the island grows as the crash proceeds. The temperature differences are shown in Fig. 9(b). The shift of the hot spot is not clear at the beginning of the crash, but a part of the hot spot extends to the region between the inversion radius and the mixing radius [see Fig. 9(b) [B],[D]]. This narrow extension is also seen in the case of a slow sawtooth crash in the NBI heated plasmas (see Fig. 3) and in the ICRH heated plasma (see Fig. 7). This extension is smaller on the inboard side [see Fig. 9(b) [C]] than on the outboard side [see Figs. 9(b) [B],[D]]. There is a noticeable warm region (surrounded by a thick contour) between the hot spot and the island [see Fig. 9(a) [E]]. The behavior of this warm region is similar to that in slow sawtooth crashes in ICRH plasmas (see Fig. 7).

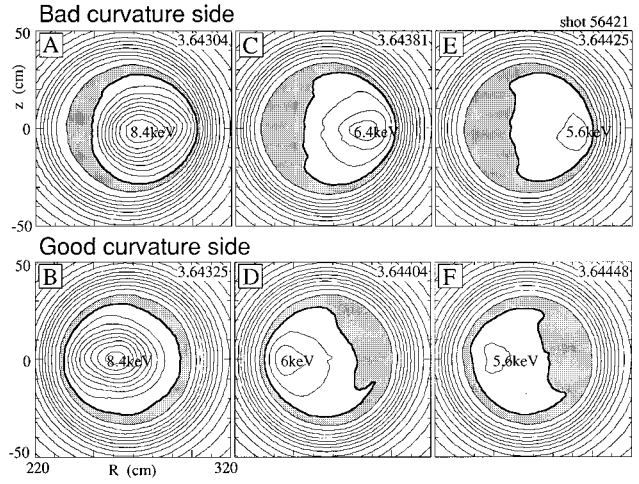

FIG. 7. Series of ECE images when the hot spot is on the bad and the good curvature sides during the slow sawtooth crash in an ICRH heated plasma. The contour step size is 400 eV. The numbers on the right shoulder of the figures indicate the reconstruction time in seconds. Absence of the ECE channel at $R=295$ cm makes a deformation in the reconstructed ECE images. The thick contour indicates $T_e=5.2$ keV. The hatched region indicates $T_e=4.8-5.2$ keV.

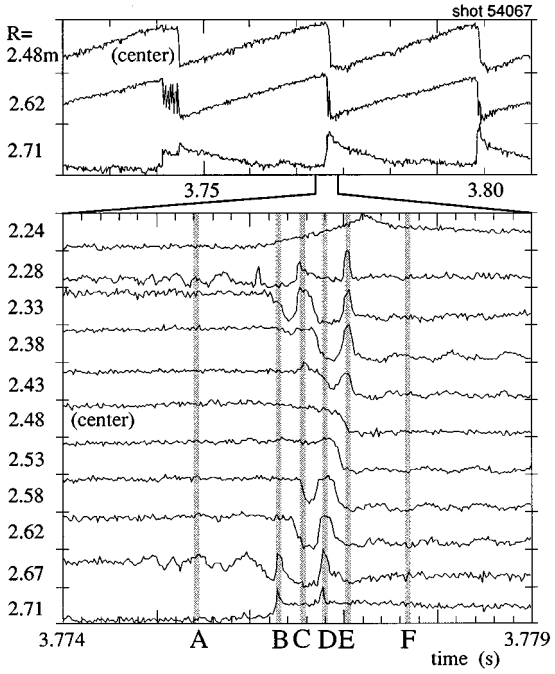

FIG. 8. ECE signals of a slow sawtooth crash in an Ohmic plasma.

III. POST-CURSOR

A slowly decaying $m=1$ mode is often observed after the sawtooth crash, this is called the ''post-cursor'' oscillation. On TFTR, just two types of post-cursors are observed; one in-phase with the precursor oscillation and the other out-of-phase with the precursor oscillation. Similar results have been obtained in the Joint European Tokamak (JET).[13] An example of an out-of-phase post-cursor is shown in Figs. 1–5. There is a noticeable cool region between the hot spot and the island. The cool region has been also observed in faster sawtooth crashes.[6] The size of the cool region does not shrink as much as the hot spot does (see Fig. 3 [F]). The $m=1$ cool region remains after the sawtooth crash. This $m=1$ cool region generates the out-of-phase post-cursor oscillation. An example of an in-phase post-cursor is shown in Figs. 6–9. The $m=1$ warm region between the hot spot and the island, which is indicated by the thick contour, remains after the sawtooth crash (see Fig. 7 [F], Fig. 9 [F]). This

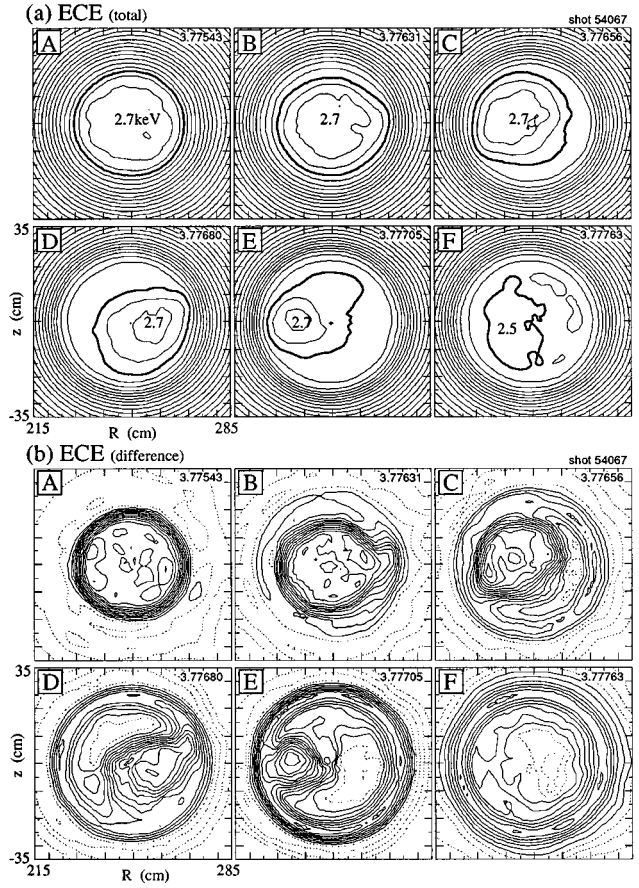

FIG. 9. (a) Series of ECE images during the slow sawtooth crash in the Ohmic plasma. The contour step size is 100 eV. The thick contour indicates $T_e = 2.5$ keV. (b) Reconstruction of the temperature difference. The contour step size is 20 eV and dotted lines indicate less than 100 eV. The numbers on the right of the figures indicate the reconstruction time in seconds. The capital letters on the left of the figures correspond to the alphabets in Fig. 8.

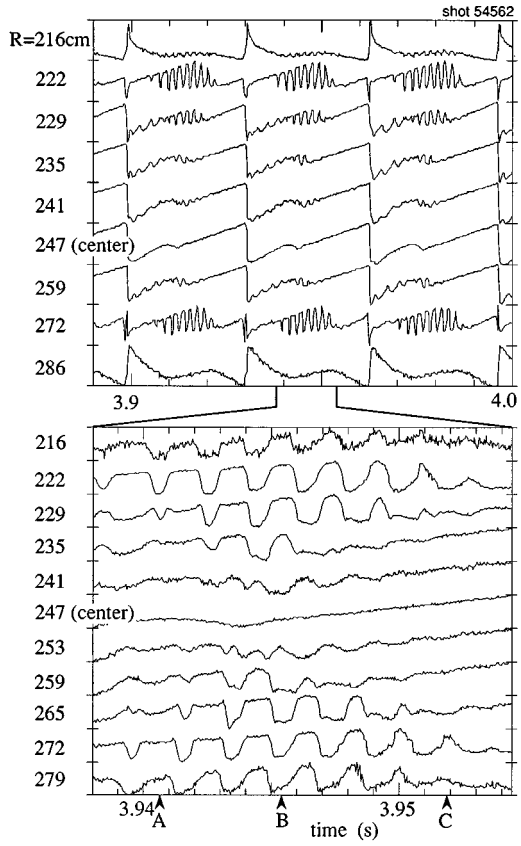

FIG. 10. ECE signals of sawteeth with mid-cursors.

$m = 1$ warm region generates the in-phase post-cursor oscillation. The cool or warm region can be explained by a reconnection process as follows: the heat is mixed up between the inside layer and the outside layer due to the reconnection; when the temperature profile has a steep gradient outside the $q = 1$ surface, the reconnected layer becomes cooler than the island region; when it has a broader profile, the reconnected layer becomes warmer.

The post-cursor cannot be explained by the full reconnection model. A second reconnection model[14] implies the post-cursor. In this model, it is stated that following the Kadomtsev phase the strong flow pulls the helical flux back into the central region.[14] Since the electron thermal diffusion is fast on the same flux surface, the electron temperature on the flux surface that is pulled back from the outside should be slightly different from that on the island region. The new region may be cool. Since the new region should be on the opposite side of the hot spot, it should generate a post-cursor oscillation. This prediction is obviously inconsistent with the TFTR data as shown in the previous paragraphs. In addition, neither cool nor hot phenomena appear on the opposite side of the hot spot in any analyzed sawtooth crashes on TFTR.

Isothermal contours represent flux surfaces as a result of the fast parallel diffusion. Therefore, the post-cursor phenomena indicate that the $m = 1$ mode and its flux surface remains after the crash. Since the size of the flux surface is determined by the amount of total current inside the flux surface, the remaining cool (see Fig. 3 [F]) or warm (see Fig. 7 [F], Fig. 9 [F]) region shows that a substantial fraction of the $m = 1$ helical current on the hot spot remains in the same place after the sawtooth crash. This result is consistent with the q-profile measurements.[3,7] This result is inconsistent with the second reconnection model,[14] which predicts that the current flows on the newly generated flux surface.

IV. MID-CURSOR

An $m = 1$ mode in the middle of the sawtooth period is observed in the Ohmic discharge. Here, this oscillation will be called the ''mid-cursor.'' An example of mid-cursor is shown in Figs. 10–11. Figure 10 shows the ECE signals of an Ohmic plasma with $\beta_p = 0.07$, $q_a = 3$, $B_t = 5.2$ T, $I_p = 2.2$ MA, $R = 245$ cm and $a = 80$ cm. After a sawtooth crash, the post-cursor occurs in the circular region of $r = 19$ cm. Following the post-cursor, a mid-cursor occurs in the ring-shaped region between $r = 16$ cm and $r = 33$ cm. In this case the inversion radius is $r = 30$ cm. The phase of the mid-cursor and the post-cursor is opposite. The wave form of the mid-cursor oscillation has the feature that the bottom of the wave is sharp and the top of the wave is flat. This is opposite to the $m = 1$ oscillation due to a hot spot (see Fig. 1). During the mid-cursor, the electron temperature at the peripheral re-

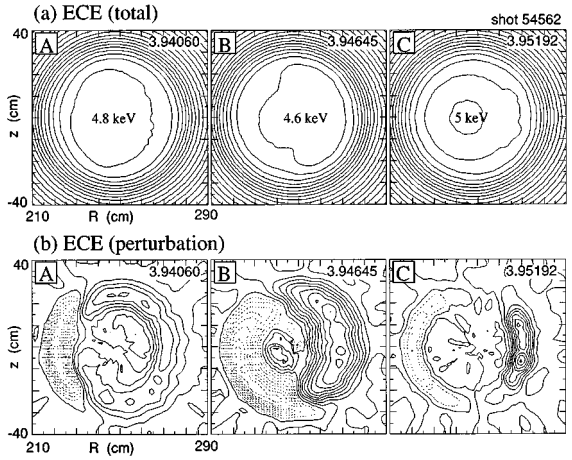

FIG. 11. (a) Series of ECE images during the mid-cursor. The contour step size is 200 eV. (b) Contour plot of perturbation in the electron temperature. The contour step size is 15 eV and dotted lines indicate negative value. The numbers on the right shoulder of the figures indicate the reconstruction time in seconds. The capital letters on the left of the figures correspond to the alphabets in Fig. 10.

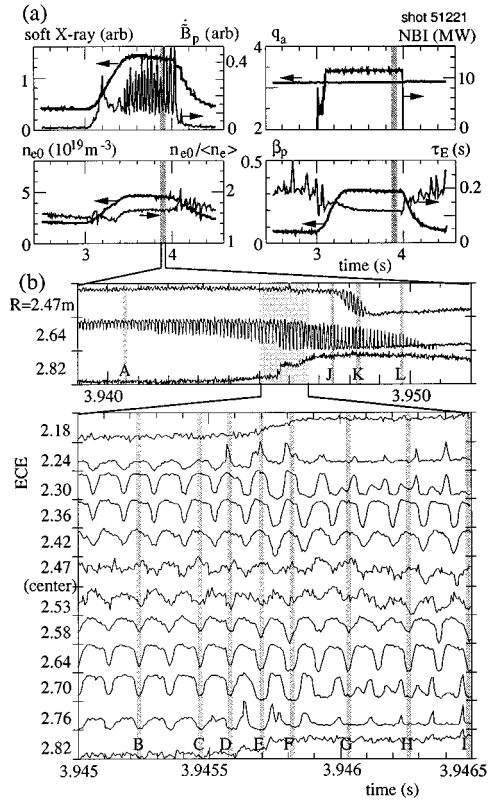

FIG. 12. (a) Time evolution of soft x-ray, poloidal field fluctuation ($\dot{\tilde{B}}$), central plasma density (n_{e0}), density peaking parameter ($n_{e0}/\langle n_e\rangle$), q_a (cylindrical), NBI power, poloidal beta (β_p) and energy confinement time (τ_E) of the sawtoothing plasma with a cold bubble. (b) ECE signals of the partial crash with a cold bubble.

gion of the inversion radius ($R=286$ cm) increases. This indicates that the mid-cursor causes the heat transfer from the ring-shaped region to the peripheral region. A series of contour plots of electron temperature profile and the perturbation on temperature are shown in Fig. 11. During the mid-cursor, the hot region shrinks and the cold region expands. This corresponds to the heat transfer from the ring-shaped region to the peripheral region. The time scale of this heat transfer is about 10 ms. The mid-cursor and the post-cursor suggest that the $q=1$ surface remains and the $m=1$ MHD instability can be active after the sawtooth crash.

V. SAWTEETH WITH COLD BUBBLE

In the Wesson model,[15] which is a 2-D model, it is explained that the kink flow draws the cold bubble into the central region and causes the fast sawtooth crash. Figures 12–14 show an example of sawteeth with a cold bubble in a beam heated plasma with $\beta_p=0.3$, $q_a=$ 3.1, $B_t=4.8$ T, $I_p=2$ MA, $R=245$ cm and $a=80$ cm. Figure 12(a) shows the time evolution of the soft x-ray, $\dot{\tilde{B}}$, n_{e0}, density peaking parameter, q_a (cylindrical), neutral beam injection (NBI) heating power, β_p and τ_E, and Fig. 12(b) shows the ECE signals. The wave form of the precursor oscillation of the partial crash has the characteristic features of a cold bubble, i.e., the bottom of the wave is sharp and the top of the wave is flat. This is opposite to the $m=1$ oscillation with a hot spot (see Fig. 1). In the post-cursor oscillation of the partial crash, ECE signals of the inner channels (for example: $R=264$ cm) have the feature of a cold bubble and ECE signals of the outer channels (for example: $R=276$ cm) have the feature of a hot spot. Finally, a very slow full crash takes place.

A series of contour plots of the electron temperature profile during the partial crash with a cold bubble are shown in Fig. 13. A series of contour plots of the temperature difference are shown in Fig. 14. These figures are arranged so that the cold bubble sits on the weak field side (the larger major radius side). A cold bubble gradually grows during a precursor oscillation (see Figs. 13, 14 [A]–[C]). A projection extends out from the hot spot on the opposite side of the cold bubble (see Fig. 14 [D]), and the heat ring is developed (see Fig. 14 [E]–[F]). This is the partial crash. Since the electron temperature profile is flat, the q-profile may be flat. The cold bubble may be enhanced because the q profile is flat.[15] The above phenomenon is consistent with the hypothesis that the kink flow makes a cold bubble and causes the reconnection on the opposite side of the cold bubble.[16] However, the cold bubble does not cause the full crash but causes the partial crash in TFTR. During the partial crash, the cold bubble expands in the poloidal direction and becomes a crescent-shaped island (see Figs. 13, 14 [D]–[F]). Both in the Wesson model[15] and in the Kolesnichenko model,[16] it is predicted that the cold bubble enters the core plasma region and is surrounded by a closed surface. These theoretical models are inconsistent with the TFTR experimental results.

At the end of the partial crash (see Figs. 13, 14 [G]), the hot spot shape becomes elongated, and another island appears on the opposite side of the cold bubble. So, the (2, 2) mode is developed after the partial crash. These two islands merge to be one island (see Figs. 13, 14 [I]–[J]). As the result of this merging, an $m=1$ island and an $m=1$ hot spot are established. Interestingly, the new hot spot and the old hot spot are separated by 90° (see Figs. 13, 14 [J]). The

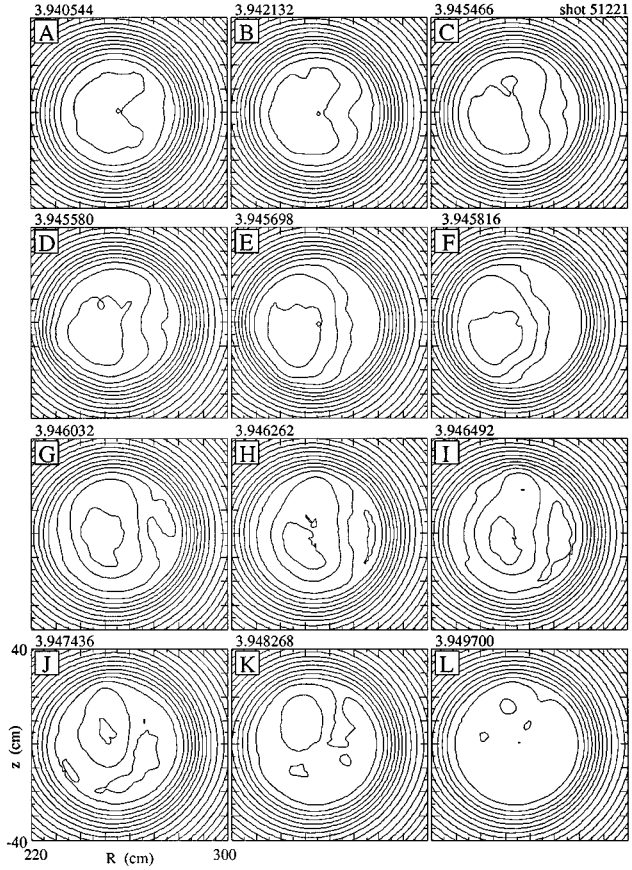

FIG. 13. Series of ECE images during the partial and full sawtooth crash with a cold bubble. The contour step size is 200 eV. The numbers on the left shoulder of the figures indicate the reconstruction time in seconds. The capital letters on the left of the figures correspond to the alphabets in Fig. 12.

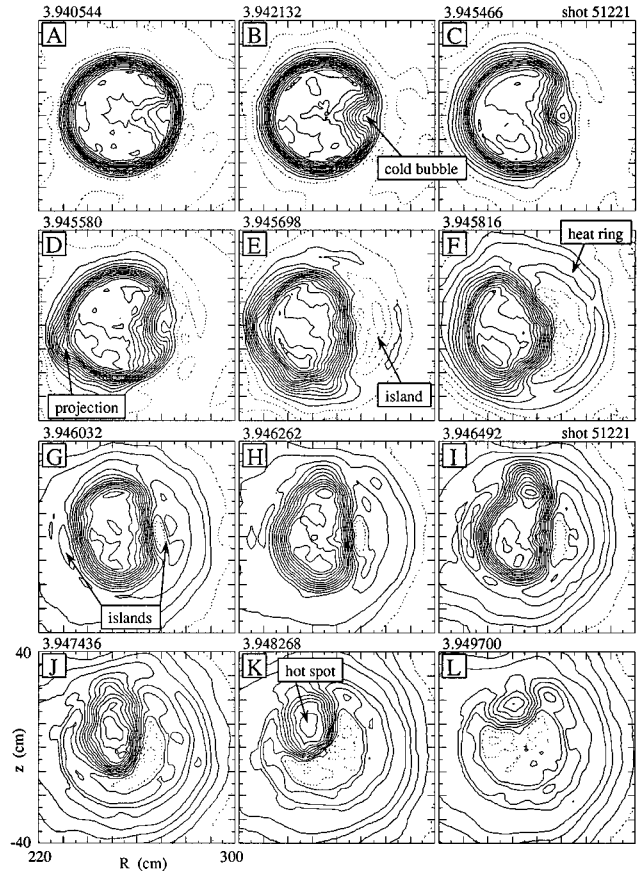

FIG. 14. Reconstruction of the temperature difference during the partial and full sawtooth crash with a cold bubble. The contour step size is 30 eV and dotted lines indicate less than 120 eV. The capital letters on the left of the figures correspond to the alphabets in Fig. 12.

merging of the islands and the creation of a new hot spot is an interesting phenomenon. As seen in a usual full crash, the $m=1$ hot spot shrinks and the full crash is eventually completed.

VI. CRASH TIME

Since the crash time is faster[17] than the Kadomtsev reconnection time, the Wesson model[15] and the electron inertia effect on the reconnection[18] have been considered. So the crash time is an important issue in the sawtooth physics. Figure 15(a) compares the observed crash time and the Kadomtsev reconnection time.[1] Figure 15(b) compares the observed crash time and the reconnection time considering the electron inertia.[18] The Kadomtsev time is slower than the observed crash time and the inertia time is faster than the observed crash time. Therefore the 2-D reconnection time is not consistent with the TFTR experiment. In Fig. 15(c), the observed crash time is plotted versus the difference between the electron temperature on the magnetic axis and that at the inversion radius. The temperature difference is almost equal to the temperature drop at the plasma center. The plot suggests that a faster crash is associated with a larger temperature drop. Recently, Haas and Thyagaraja proposed a crash time scaling based on a turbulence model.[19] In Fig. 15(d), the

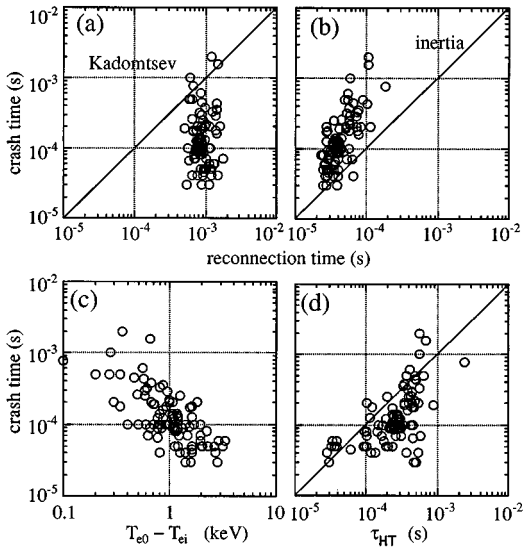

FIG. 15. (a) Comparison of the observed crash time and the Kadomtsev reconnection time.[1] (b) Comparison of the observed crash time and the reconnection time considering the electron inertia. [18] (c) The observed crash time versus the difference between electron temperature at the magnetic axis and at the inversion radius. (d) Comparison of the observed crash time and Haas and Thyagaraja's crash time scaling (τ_{HT}).[19]

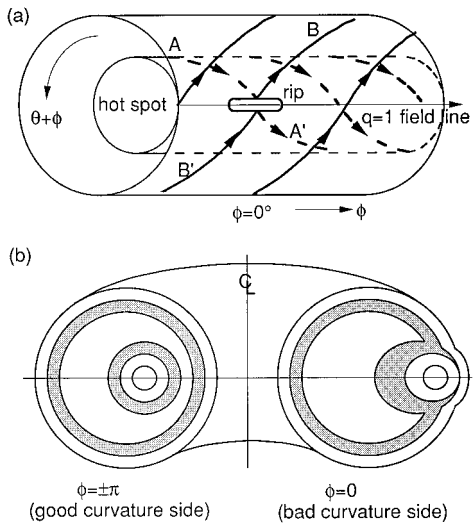

FIG. 16. (a) Schematic view of the localized reconnection during a sawtooth crash. We use the helical coordinates with the helicity of $q=1$ $(\theta+\phi, \phi)$, so that the $q=1$ line is straight. Dotted line indicates the field line on the inside surface and solid line those on the outside surface. The inside field line A-A′ is reconnected to the outside field line B′-B. (b) Flux surfaces on the good curvature side ($\phi=0°$) and on the bad good curvature side ($\phi=180°$). The rip is located at $\phi=0°$. The dark region indicates the reconnected region.

observed crash time is plotted versus their crash time scaling. This scaling gives better agreement than the Kadomtsev model.

VII. DISCUSSION

Previously proposed 2-D models[1,14–16,18] cannot explain the experimental results in TFTR. Since the localized reconnection cannot be treated with a 2-D model, we consider a 3-D model[20] for the sawtooth crash. Reconnection points form a line with a helicity of $q=1$. Hereafter, we call this line a ''rip''. Figure 16(a) shows a schematic picture of the field line reconnection at a rip in the helical coordinates $(\phi, \phi+\theta)$, where ϕ and θ are the toroidal and poloidal angles, respectively. Suppose the field line A-A′ inside the $q=1$ surface and the field line B′-B outside the surface are reconnected to be lines A-B and A′-B′ at the rip. In the 2-D reconnection model[1] the rip surrounds the torus, so that all field lines on the surface of the hot spot must be reconnected to the field line outside the $q=1$ surface. In the case of a localized reconnection, however, the rip is localized on the bad curvature side, and a small area of field is reconnected. Basically one field line nests a flux surface, thus all particles and heat can quickly escape along the reconnected field line through the rip, even if it is localized. Since the localized reconnection process does not destroy the whole flux surface, substantial amounts of the $m=1$ flux surface or the $m=1$ helical current should be preserved. Therefore, the localized reconnection is the fast heat transport mechanism without the q-profile change.

A speculative explanation of the sawtooth crash now emerges. First, the $m=1$ mode grows, making a steep pressure gradient at the X-point. Eventually the pressure gradient exceeds the local threshold of the ballooning mode, and the crash begins; the ballooning mode makes a localized short rip, the heat and particles quickly escape along the reconnected field line. Note that the ballooning mode, once destabilized, does not stop easily because the ballooning mode itself makes the pressure gradient steeper.[21] Finally, the resultant wide, flat temperature region, which now extends to the mixing radius, stabilizes the ballooning mode, and the sawtooth crash process stops. The remaining $m=1$ mode is responsible for the post-cursor oscillation. The $m=1$ mode is stabilized after the crash on a slower time scale.

The localized reconnection model agrees well with the TFTR experiments. The significant in-out asymmetries (see Figs. 2, 5), the narrow perturbation and the radially elongated hot spot shape (see Fig. 3) suggest that the reconnection is localized in both poloidal and toroidal directions. The similar in-out asymmetry is also observed in Ohmic plasmas (see Fig. 9). This is a basic assumption of this model. Figures 3 and 7 show the preservation of the $m=1$ helical flux surface, which is an important prediction of this model. This model is also consistent with the experimental result that $q_0<1$ after the crash.[7] Since the q profile does not change in this model, the $m=1$ MHD instability can be active after the crash. This prediction is consistent with the observed mid-cursor phenomena (see Figs. 10–11). The localized reconnection rate may be different from the full reconnection rate, because the localized reconnection is not accompanied by a large poloidal flux change.

The observed ballooning mode in high β TFTR plasmas is toroidally localized on the bad curvature side.[22,23] These features are consistent with a 3-D MHD simulation result.[21] Theoretical studies have shown that the ballooning mode can be excited due to the nonlinear growth of the low n kink mode.[21,24] Therefore, we can assume the ballooning mode is excited at the boundary of the hot spot and the $q=1$ surface and it causes the reconnection at the toroidally localized position on the bad curvature side.

The driven reconnection is experimentally observed.[25] When the reconnection is driven by an instability, the reconnection rate may depend on the growth rate of the instability. Here we have assumed that the hot spot shift caused by the $m=1$ mode produces the steep pressure gradient and thus destabilizes the instability on the bad curvature side. In this case, the larger temperature difference between the magnetic axis and the $q=1$ surface can cause a more violent instability. This discussion may explain the observed tendency in the sawtooth crash time (see Fig. 15).

VIII. CONCLUSION

In conclusion, an experiment using an ECE image reconstruction during the full sawtooth crash in TFTR plasmas shows that the reconnection takes place on the bad curvature side, that the hot spot shape is consistent with a ballooning mode, and that the flux surfaces of the original hot spot remain. The TFTR experimental results are not consistent with 2-D models. A possible mechanism for the sawtooth crash is a 3-D localized reconnection. This process explains the fast heat and particle transfer which keeps the condition $q_0<1$. This model agrees well to the sawtooth crash not only in

high β plasmas but also in low β plasmas. The localized reconnection is also useful to explain the partial sawtooth crash considering the mode structure.[26] The confirmation of this model on the fast sawtooth crashes in ICRH plasmas and in L-mode plasmas remains a subject for future work.

ACKNOWLEDGMENTS

The authors would like to thank Dr. J. Manickam for useful discussions. The authors would also like to acknowledge the TFTR group for their operational and diagnostic support and for useful discussions.

This work was supported by the U. S. Department of Energy under Contract No. DE-AC02-76-CHO-3073.

[1]B. B. Kadomtsev, Fiz. Plazmy **1,** 710 (1975) [Sov. J. Plasma Phys. **1,** 389 (1975)].
[2]C. Janicki, R. Decoste, and C. Simm, Phys. Rev. Lett. **62,** 3038 (1989).
[3]H. Soltwisch, Rev. Sci. Instrum. **59,** 1599 (1988).
[4]M. Yamada, *Recent Experiments on Magnetic Reconnection in Laboratory Plasmas* AGU Monograph, edited by P. Song, B. Sonnerup, and M. Thomsen (American Geophysical Union, Washington, DC, 1995) pp. 215–223.
[5]H. Baty, J. F. Luciani, and M. N. Bussac, Phys. Fluids B **5,** 1213 (1993).
[6]Y. Nagayama, K. M. McGuire, M. Bitter, A. Cavallo, E. D. Fredrickson, K. W. Hill, H. Hsuan, A. Janos, W. Park, G. Taylor, and M. Yamada, Phys. Rev. Lett. **67,** 3527 (1991). For general information on TFTR see R. J. Hawryluk, V. Arunasalam, C. W. Barnes, M. Beer, M. Bell, R. Bell, H. Biglari, M. Bitter, R. Boivin, N. L. Bretz, R. Budny, C. E. Bush, C. Z. Cheng, T. K. Chu, S. A. Cohen, S. Cowley, P. C. Efthimion, R. J. Fonck, E. Fredrickson, H. P. Furth, R. J. Goldston, G. Greene, B. Grek, L. R. Grisham, G. Hammett, W. Heidbrink, K. W. Hill, J. Hosea, R. A. Hulse, H. Hsuan, A. Janos, D. Jassby, F. C. Jobes, D. W. Johnson, L. C. Johnson, J. Kesner, C. Kieras-Phillips, S. J. Kilpatrick, H. Kugel, P. H. La Marche, B. LeBlanc, D. M. Manos, D. K. Mansfield, E. S. Marmar, E. Mazzucato, M. P. McCarthy, M. Mauel, D. C. McCune, K. M. McGuire, D. M. Meade, S. S. Medley, D. R. Mikkelsen, D. Monticello, R. Motley, D. Mueller, Y. Nagayama, G. A. Navratil, P. Nazikian, D. K. Owens, H. Park, W. Park, S. Paul, F. Perkins, S. Pitcher, A. T. Ramsey, M. H. Redi, G. Rewoldt, D. Roberts, A. L. Roquemore, P. H. Rutherford, S. Sabbagh, G. Schilling, J. Schivell, G. L. Schmidt, S. D. Scott, J. Snipes, J. Stevens, B. C. Stratton, W. Stodiek, E. Synakowski, Y. Takase, W. Tang, G. Taylor, J. Terry, J. R. Timberlake, H. H. Towner, M. Ulrickson, S. von Goeler, R. Wieland, M. Williams, J. R. Wilson, K. L. Wong, M. Yamada, S. Yoshikawa, K. M. Young, M. C. Zarnstorff, and S. J. Zweben, Plasma Phys. Controlled Fusion **33**, 1509 (1991).
[7]F. M. Levinton, S. H. Batha, M. Yamada, and M. C. Zarnstorff, Phys. Fluids B **5,** 2554 (1993).
[8]M. Yamada, F. M. Levinton, N. Pomphrey, R. Budny, J. Manickam, and Y. Nagayama, Phys. Plasmas **1,** 3269 (1994).
[9]A. Cavallo, R. C. Cutler, and M. P. McCarthy, Rev. Sci. Instrum. **59,** 889 (1988).
[10]Y. Nagayama, Rev. Sci. Instrum. **65,** 3415 (1994).
[11]M. Yamada, Y. Nagayama, W. Davis, E. Fredrickson, A. Janos, and F. Levinton, Rev. Sci. Instrum. **63,** 4623 (1992).
[12]W. Park, D. A. Monticello, E. Fredrickson, and K. McGuire, Phys. Fluids B **3,** 507 (1991).
[13]Y. Nagayama and A. W. Edwards, Rev. Sci. Instrum. **63,** 4757 (1992).
[14]D. Biskamp and J. F. Drake, Phys. Rev. Lett. **73,** 971 (1994).
[15]J. A. Wesson, Plasma Phys. Controlled Fusion **28,** 243 (1986).
[16]Ya. I. Kolesnichenko, Yu. V. Yakovenko, D. Anderson, M. Lisak, and F. Wising, Phys. Rev. Lett. **68,** 3881 (1992).
[17]A. W. Edwards, D. J. Campbell, W. W. Engelhardt, H.-U. Fahrbach, R. D. Gill, R. S. Granetz, S. Tsuji, B. J. D. Tubbing, A. Weller, J. Wesson, and D. Zasche, Phys. Rev. Lett. **57**, 210 (1986).
[18]J. A. Wesson, Nucl. Fusion **30,** 2545 (1990).
[19]F. A. Haas and A. Thyagaraja, Plasma Phys. Controlled Fusion **37,** 415 (1995).
[20]Y. Nagayama, ''Localized reconnection model for sawtooth crash,'' submitted to J. Plasma Fusion Res. (in Japanese).
[21]W. Park, E. D. Fredrickson, A. Janos, J. Manickam, and W. M. Tang, Phys. Rev. Lett. **75,** 1763 (1995).
[22]Y. Nagayama, S. A. Sabbagh, J. Manickam, E. D. Fredrickson, M. Bell, R. V. Budny, A. Cavallo, A. C. Janos, M. Mauel, K. M. McGuire, G. A. Navratil, G. Taylor, and M. Yamada, Phys. Rev. Lett. **69**, 2376 (1992).
[23]Y. Nagayama, M. Yamada, S. A. Sabbagh, J. Manickam, E. D. Fredrickson, M. Bell, R. V. Budny, A. Cavallo, A. C. Janos, M. Mauel, K. M. McGuire, G. A. Navratil, and G. Taylor, Phys. Fluids B **5,** 2571 (1993).
[24]M. N. Bussac and R. Pellat, Phys. Rev. Lett. **59,** 2650 (1987).
[25]M. Yamada, Y. Ono, A. Hayakawa, M. Katsurai, and F. W. Perkins, Phys. Rev. Lett. **65,** 721 (1990).
[26]Y. Nagayama, G. Taylor, M. Yamada, E. D. Fredrickson, A. C. Janos, and K. M. McGuire, ''ECE image reconstruction of partial sawtooth crashes in ohmic plasmas,'' Nucl. Fusion (in press).